Influence of surface acoustic waves on lateral forces in scanning force microscopies

G. Behme
Paul Drude Institute for Solid State Electronics, Hausvogteiplatz 5–7, D–10117 Berlin, Germany

T. Hesjedal[a)]
Solid State and Photonics Lab, Stanford University, Stanford, California 94305-4075

(Received 7 August 2000; accepted for publication 14 February 2001)

We present a detailed study of the influence of ultrasonic surface acoustic waves (SAWs) on point-contact friction. Lateral force microscopy (LFM) and multimode scanning acoustic force microscopy (SAFM) were used to measure and to distinguish between the influence of in-plane and vertical surface oscillation components on the cantilever's torsion and bending. The experiments show that friction can locally be suppressed by Rayleigh-type SAWs. Through the mapping of crossed standing wave fields, the wave amplitude dependence of the friction is visualized within microscopic areas without changing other experimental conditions. Above a certain wave amplitude threshold, friction vanishes completely. We found that the friction reduction effect is caused by the vertical oscillation components of the SAW. Purely in-plane polarized Love waves do not give rise to a significant friction reduction effect. Thus, we conclude that the mechanical diode effect, i.e., the effective shift of the cantilever off of the oscillating surface, is responsible for the SAW-induced lubrication. This explanation is supported by vertical and lateral SAFM measurements: in areas with completely vanishing friction, low frequency vertical cantilever oscillations are still observable, whereas lateral (torsional) cantilever oscillations are no longer excited. Additionally, at very high Rayleigh wave amplitudes an effect of lateral force rectification was observed. It results in a scan direction-independent appearance of the LFM traces. [DOI: 10.1063/1.1362413]

I. INTRODUCTION

For industrial applications, the main tribological concern is to reduce the friction coefficient, and by that the dissipated energy. Therefore, the investigation of controlled friction reduction is of great basic as well as technological interest. The common way of controlling friction is the choice of special materials combinations and the use of lubricants. However, it is a well known fact that vibrations ease the motion of bodies, e.g., for loosening a screw or the movement of an object off of a vibrating table. In the pioneering work of Fridman and Levesque, the reduction of static friction by sonic vibrations was first described.[1] Further investigations[2,3] led, for instance, to the development of a positioning device for electron microscopes.[4] There, friction made it difficult to keep the sample's position after small movements due to reversible elastic forces. Using common lubricants on the other hand had the disadvantage of slipping of the stage due to vibrations. Ultrasound was found as a helpful tool to overcome those problems, since it allows the control of friction by varying the acoustic amplitude.

Recently, ultrasound-induced lubrication was also reported in microscopic contacts,[5] studied by scanning force microscopy. However, several effects may account for the friction reduction effect, which are impossible to be clearly identified without a precise source of acoustic vibration.[6] In bulk and shear wave transducers parasitic surface displacements due to the existence of boundaries, the actual substrate cut, and the sample attachment by gluing, can hardly be avoided. These problems can be overcome by employing surface acoustic waves (SAWs). They offer the most superior source of well-defined surface oscillations with a perfectly determined polarization. In this article we present measurements of the influence of SAWs on lateral forces acting on the microscopic tip-sample contact.

II. SURFACE ACOUSTIC WAVE SAMPLE DESIGN AND FABRICATION

In order to study the effect of ultrasound on point-contact friction, we employed surface acoustic waves as a source of surface oscillations. As SAWs are acoustic modes that are confined within a wavelength to the surface of a solid and propagate along specific crystalline directions, the wave field can be easily excited, measured, and modified by means of a surface patterning. For our purposes, another advantage is even more important: SAWs lead to extremely well-defined trajectories of the excited surface elements.

Here, we focused primarily on Rayleigh-type SAWs and for comparison on Love waves. Rayleigh-type waves are predominantly polarized in the sagittal plane that is formed by the SAW propagation direction and the vector normal to the surface, i.e., the surface oscillates on elliptical trajectories with a large vertical and a smaller lateral oscillation component (Fig. 1, left-hand side). The transversally polarized

[a)]Author to whom correspondence should be addressed; electronic mail: thorsten@snow.stanford.edu

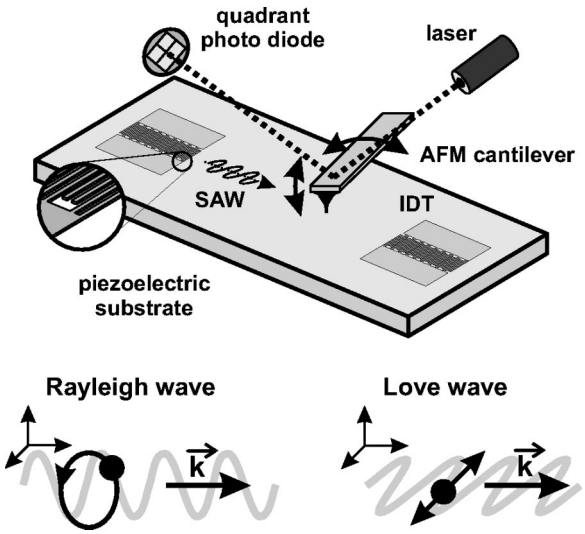

FIG. 1. Experimental setup: SAWs, which are generated by IDTs, propagate towards the LFM/SAFM scan area. For SAFM, up to four slightly detuned rf SAWs are mixed at the nonlinearity of the tip-sample contact, giving rise to vertical and lateral cantilever oscillations at the difference frequency. Additionally, the displacement components for Rayleigh and Love waves are displayed. The Rayleigh-type wave is predominantly polarized in the sagittal plane, whereas the Love wave has an in-plane (transverse) oscillation component only.

Love waves, on the other hand, have solely an in-plane oscillation component perpendicular to the propagation vector (Fig. 1, right-hand side), and will be employed to additionally distinguish between the effect of in-plane and vertical oscillation components on the local friction. Both types of waves can be excited using interdigital transducers (IDTs) on specific layered piezoelectric substrate systems, such as ST cut quartz with a fused silica overlayer. Further overlayers, such as metal films, can also be used to alter the SAWs propagation properties.

For the study of the effects of SAWs on friction, special IDTs have been designed for the excitation of Rayleigh and Love waves. The structures were fabricated by photolithography on GaAs[110](001) and on ST cut quartz substrates. On these materials generalized Rayleigh-type SAW modes can be efficiently excited with IDTs. For our investigations, five different types of SAW devices were designed. On GaAs, splitfinger IDTs were fabricated at 198 MHz, corresponding to a wavelength of 14.4 μm, in form of a single and a crossed delay line configuration. Each single line consists of two IDTs with 1400 electrode fingers. This assures a good electrical matching and a low insertion loss, thus providing decent SAW amplitudes at low rf input power. The next two devices are based on single finger IDTs at 538 MHz (1000 electrodes) on GaAs ($\lambda = 5.2$ μm), with standard and particular short electrodes. The latter ones allow the measurement across the entire SAW beam in a single microscope scan at the cost of poorer electrical performance. As a reference sample a 14.4 μm wavelength delay line was fabricated on ST quartz with 90° propagation direction with respect to the crystal's *X* axis. The entire device was covered with a 200 nm SiO_2 layer that allows for the excitation of Love waves at a frequency of about 348 MHz. All devices have been electrically characterized using a rf probe station and a vector network analyzer. They exhibit typical unmatched insertion losses between 20 and 30 dB. For our investigations, the devices were wire bonded and mounted onto the sample stage. Continuous wave or amplitude-modulated rf power was applied to the IDTs without additional matching.

III. EXPERIMENTAL TECHNIQUES AND FRICTION REDUCTION EFFECT

All experiments were performed in air at room temperature using a commercial multimode scanning force microscope,[7] capable of the simultaneous acquisition of topography and lateral force microscopy signal. All-silicon cantilevers[8] were employed in the experiments. The cantilever deflection in response to forces acting on the atomic force microscopy (AFM) tip is picked up via a standard beam-bounce technique, where a laser spot is reflected off the very end of the cantilever towards a quarter-segmented photo detector. A sketch of the general experimental setup, consisting of the force microscope, the piezoelectric sample, and IDTs for the SAW excitation, is shown in Fig. 1. The optical detector delivers signals proportional to the deviation from the cantilever's rest position in the vertical and the lateral direction.[9] The latter one delivers the lateral force microscopy (LFM) signal that reflects the torsion of the cantilever due to friction or steep topographical features.[10] The cantilever is twisted around its rest position by forces counteracting the movement of the scanned tip. The pristine LFM trace exhibits a more or less pronounced hysteresis effect between forward and backward scan direction, depending on the interacting materials, scan speed, force setpoint and tip geometry, as well as the temperature and humidity of the environment. The LFM mode is commonly applied as a tool for the visualization of variations in local friction[11] due to a phase or material contrast. Here, it will be applied to visualize the effects of local reduction of friction.

A. Scanning acoustic force microscopy

The scanning acoustic force microscope (SAFM)[12] is used to detect the amplitude and phase of ultrasonic surface acoustic waves down to submicron lateral regions, employing a conventional AFM setup (see Fig. 1). Since typical cantilever resonance frequencies are of the order of 100 kHz, the cantilever cannot follow the high frequency surface oscillations. However, due to the nonlinear force-to-distance dependence, the cantilever's rest position is effectively shifted away from the surface. Employing this mechanical diode effect,[13] an acoustic oscillation can be self-mixed, or mixed with another acoustic wave, delivering an amplitude-proportional signal or the phase of the acoustic wave.[14] In particular, the amplitude is measured by picking up the vertical deflection signal due to an amplitude-modulated rf SAW and analyzing it with a lock-in amplifier at the modulation frequency. The modulation frequency is typically chosen to be below the cantilever contact resonance frequency but above the frequency response of the *z*-feedback loop of the AFM.

Figure 2(a) shows the topography (lower left triangle) and the SAFM amplitude image (upper right triangle) of the corresponding area close to the aperture of a SAW trans-

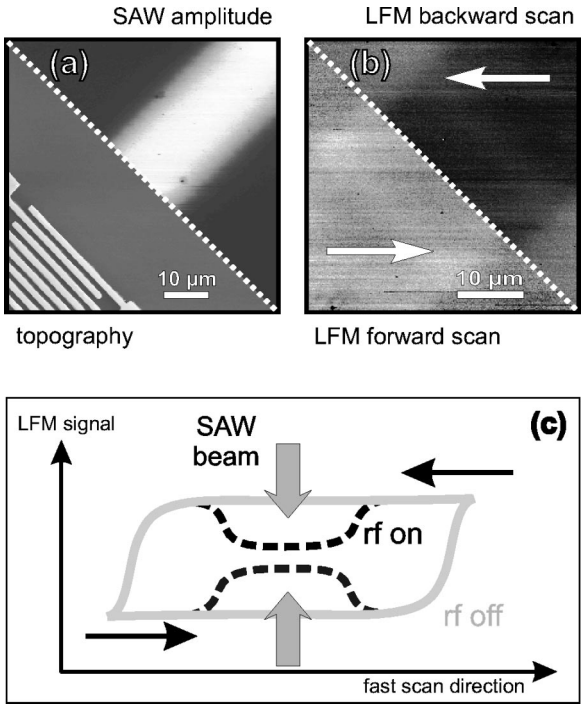

FIG. 2. (a) 60 μm AFM topography scan of the 538 MHz IDT (lower triangle) and corresponding SAFM amplitude image (upper triangle), showing the acoustic beam launched from the transducer (bright area). (b) 40 μm LFM scan (forward scan: lower triangle; backward scan: upper triangle) across a different position of the propagating SAW beam. (c) Illustrates the observed lubrication effect: the scan direction dependent hysteresis is significantly reduced at the position of the SAW beam.

ducer. The 60 μm scan images reveal the electrodes of the 538 MHz IDT and the launched SAW beam (bright area). The SAW beam has a width of roughly 20 μm, which is given by the overlap of the interdigitated fingers of different polarity.

A technological extension of the SAFM, the lateral force mode SAFM (LFM–SAFM), allows the detection of in-plane polarized SAWs with equal lateral resolution.[15] While in conventional SAFM the additional contributions to the cantilever *bending* due to the mechanical diode effect are analyzed, the analysis of the *torsional* response to SAWs opens up a unique way to study purely in-plane oscillation components (see Fig. 1). A similar nonlinear mechanism as for the detection of vertical oscillations, namely a lateral nonlinear mechanical coupling mechanism, allows the extraction of a SAW amplitude-dependent signal. Thus, the LFM–SAFM will be applied to investigate the contrast between vertical and lateral coupling when analyzing Rayleigh waves, as these contain in- and out-of-plane oscillation components.

B. Friction reduction effect

Investigating the propagating SAW beam, for which the amplitude image was shown in the previous section, with lateral force microscopy, we found that friction was locally reduced[16] over the beam area. The LFM measurement illustrating this friction reduction effect is presented in Fig. 2(b): the lower triangle shows the forward scan and the upper triangle the backward scan [note: smaller scan size compared to Fig. 2(a)]. Both 40 μm images were recorded simultaneously with a resolution of 256×256 points, at a scan frequency of 0.2 Hz and with an overscan of 5% of the image size.

The 40 μm scan was performed across the propagating SAW beam in the vicinity of the SAW transducer, revealing an increased LFM signal across the actual beam in the forward direction and a decreased signal in the backward scan, i.e., the lateral force acting on the tip decreases in both directions. In other words, the pristine LFM hysteresis is locally reduced by the SAW beam. Note that the rf voltage was not amplitude modulated.

A sketch of the line scans with and without SAW beam illustrates the lubrication effect [Fig. 2(c)]. The undisturbed LFM trace (gray solid line) depicts the typical LFM hysteresis. Switching the SAW on leads at the beam position to a localized shift of the LFM traces (dashed lines) towards the line of zero lateral force, i.e., the characteristic LFM scan direction dependent hysteresis is significantly reduced. This friction reduction effect was observed for a variety of materials, and at frequencies ranging from 200 MHz to 3 GHz.

IV. EXPERIMENTAL STUDY OF THE FRICTION REDUCTION EFFECT

In this section, a more detailed experimental study of the friction reduction effect is presented. The influence of a crossed standing Rayleigh wave field on local friction was investigated. Also, the implications of the effect on the nonlinear mechanical coupling in both operating modes were analyzed.

A. Investigation of crossed Rayleigh wave fields

Launching counter propagating waves from two opposing IDTs establishes a standing wave field with a periodicity of half of the wavelength. For the 198 MHz Rayleigh wave devices on GaAs this yields $\lambda/2=7.2$ μm. Due to the fourfold symmetry of the (001) surface, crossed standing wave fields can easily be excited. Figure 3 shows a crossed beam arrangement of IDTs on the GaAs surface. In Fig. 3(a), the corresponding standing wave field pattern obtained by a SAFM amplitude measurement (in normal detection mode) is shown. It reveals an eggbox-like pattern (raw data, no filtering procedures applied) with an antinode periodicity of $\lambda_{SAW}/2$ in two spatial directions. As only two rf generators were used to power three of the IDTs (the fourth acts as a reflector for the opposing IDT), the modulation is less pronounced along the x axis. Figures 3(b) and 3(c) are the corresponding LFM scans in forward (left to right), and backward (right to left) scan direction, respectively. In the forward scan direction, the LFM image basically reproduces the eggbox pattern, i.e., the areas of high wave amplitude show up as areas of increased LFM signal, whereas in the backward scan direction the image appears inverted [the rings indicate the same positions in (a)–(c)]. Again, the reason is the existence of a pronounced effect of locally reduced friction. This leads to a smaller LFM hysteresis, appearing as an increase in the LFM signal (bright spots) in the forward

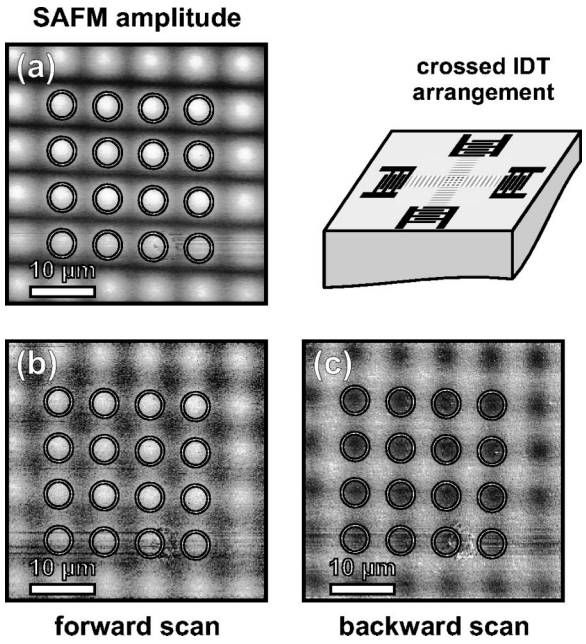

FIG. 3. SAFM amplitude image (a) and LFM scans [forward (b) and backward (c)] of a two-dimensional standing Rayleigh wave field on GaAs. The LFM images reveal the spatially distributed lubrication effect on the LFM hysteresis. The rings indicate corresponding sample positions.

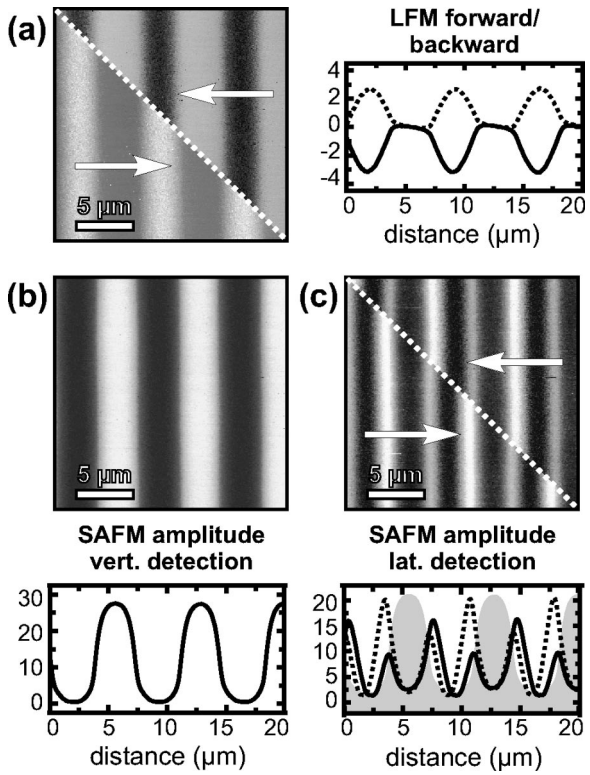

FIG. 4. (a) LFM signal (forward+backward scan), (b) vertical (normal) SAFM amplitude signal, and (c) LFM-SAFM (lateral) amplitude signal (forward+backward scan). Around the standing wave field antinodes [bright areas in (b)], friction is reduced [flat areas in (a)]. In the lateral LFM–SAFM image (c), minima appear around the antinodes which are accompanied by two side maxima.

and a decrease (dark spots) in backward scan direction, at the position of maximum oscillation amplitude [see Fig. 2(c)].

B. Investigation of the nonlinear mechanical coupling mechanism

Next, measurements on the dependence of the nonlinear mechanical coupling mechanism on friction are presented. This is of particular interest for SAFM and LFM–SAFM as the nonlinear behavior, that leads to a mechanical diode effect for vertical vibrations, is hardly understood for the coupling into cantilever torsion. Varying friction, however, allows the tuning of the lateral coupling strength. For that purpose, a standing Rayleigh wave field was excited on GaAs at 198 MHz. A rf power of 5 dBm was chosen such that the effect of vanishing friction occurs around the wave field maxima and the LFM hysteresis is still in effect elsewhere (see previous section).

Figure 4 shows the LFM image (a) (amplitude modulation turned off), along with the normal (vertical) SAFM measurement (b) and the lateral LFM–SAFM image (c). Additionally, representative line traces are shown (averaged over ten lines). The forward scans (right to left) are represented by solid lines, and the backward scans (left to right) as dashed lines. In areas of high vertical oscillation amplitude (wave field maxima), the normal SAFM amplitude image shows a maximum. Examining the LFM traces [Fig. 4(a)], it is apparent that in these areas friction is completely suppressed. This correspondence leads to the suggestion that friction is reduced via the additional quasistatic shift of the cantilever as a response to vertical rf surface oscillations, i.e., the mechanical diode effect. The absence of friction does, however, not affect the *vertical* nonlinear mechanical coupling mechanism, i.e., the normal SAFM imaging.

The standing wave field pattern that one would expect to find in the LFM–SAFM image (c) is actually the same as in the vertical SAFM image (b) (this experimental finding will be explained later). Indeed, at lower rf power, where the friction is not completely suppressed, the same behavior as in the normal SAFM is observed. However, in Fig. 4(c), minima appear at the positions of maximum amplitude, accompanied by two high signal sidelobes at lower wave amplitudes. This means that in the absence of friction, the nonlinear *lateral* mechanical coupling into the cantilever torsion breaks down. The difference between the forward and the backward scan direction in Fig. 4(b) is most likely due to the influence of the actual tip shape.

The reason for the SAFM and LFM–SAFM both responding primarily to the vertical oscillation component is that the nonlinear lateral coupling strength was found earlier to be about at least one order of magnitude smaller than the vertical coupling.[17] Thus, the tip experiences the vertical vibration of the surface only and is hardly sensitive to the 90° shifted maxima of the longitudinal component of the standing wave field (in case of Rayleigh waves), i.e., another *effective* lateral coupling mechanism must exist. The most proximate route to the torsional response to vertical oscillations lies in the friction-induced quasistatic torsion during scanning, which reflects in the LFM hysteresis. This inherently transfers a vertical movement of the surface into an additional torsion of the cantilever. Thus, it becomes evident that if the hysteresis breaks down at high wave amplitudes,

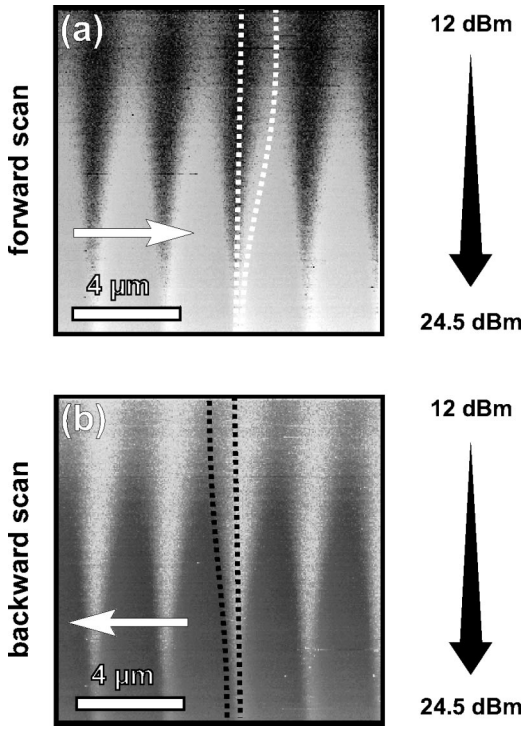

FIG. 5. 12 μm LFM scans on the 538 MHz sample: (a) forward and (b) backward scan direction. Along the *y* axis, the rf power was tuned from 12 to 24.5 dBm in steps of 0.5 dBm/ten lines. At low rf power, the hysteresis offset is very pronounced. Around 16 dBm, friction vanishes at the antinodes of the wave field. At high rf power, a scan direction independent signal remains, which is slightly shifted with respect to the low power extremes. The dashed lines indicate the apparent movement of the extremes.

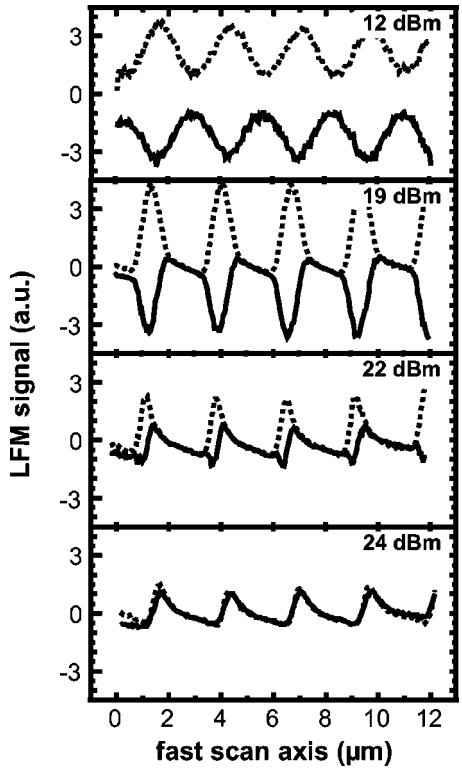

FIG. 6. LFM image of the 538 MHz sample (lower surface: forward scan, upper surface: backward scan). The rf power is tuned from 12 to 24.5 dBm. The line scans below represent four distinct interaction regimes.

an *effective* lateral coupling is no longer possible. The tip is then solely oscillating in the vertical direction. In summary, the vertical nonlinear coupling remains still active without friction present in the system, while the *effective* lateral nonlinear coupling breaks down.

V. SAW AMPLITUDE-DEPENDENT LFM CONTRAST

In this section, the SAW amplitude dependence of the LFM signal is presented. Tuning the driving power over a certain range leads to four interaction regimes that will be discussed qualitatively in detail. At high power, an effect of lateral rectification was found that leads to a scan direction-independent LFM contrast.

A. Experimental results

For the measurement of the wave amplitude dependence of the LFM signal, we employed a Rayleigh wave delay line on GaAs operating at 538 MHz. In this experiment only one IDT was powered, while the opposing one acts as a reflector. As the second IDT was electrically shorted, its reflectivity is high enough to establish a standing wave field between the transducers which is almost completely modulated. LFM images have been acquired between the IDTs at a line scan rate of 1 Hz at 256×256 points resolution (Fig. 5). Along the *y* axis, the power was tuned from 12 to 24.5 dBm in steps of 0.5 dBm per ten scan lines. Figure 5(a) shows the forward scan direction (left to right) and Fig. 5(b) the backward scan direction (right to left), respectively. Comparing both scans at low input power, it is obvious that the contrast is inverted and that the overall signal has opposite sign, that is, the LFM signal shows the typical hysteresis as described earlier. With increasing power ($\geqslant$16 dBm), the LFM signal between the maxima in both scan directions becomes identical and almost zero, i.e., friction is strongly suppressed. These areas are in the vicinity of the antinodes of the wave field. At very high input power, the overall signal becomes almost identical for both scan directions, indicating the complete suppression of friction. However, a periodic peak occurs, that is furthermore identical for both scan directions and also shifted with respect to the positions of the initial signal maxima. It starts developing at around 22 dBm and can be attributed to a lateral mechanical diode effect, i.e., an additional quasi-static cantilever torsion due to longitudinal oscillation components in areas of suppressed friction.

The graphs in Fig. 6 show the LFM linescans at applied powers of 12, 19, 22, and 24 dBm, representing four distinct interaction regimes. The *y*-axis scale (in arbitrary units) is identical throughout all graphs. Each line represents the average over ten scans.

At 12 dBm, the hysteresis offset between forward (solid line) and backward (dashed line) scan is very pronounced. However, the overall hysteresis is already slightly reduced compared to the behavior in absence of the SAW field. Again, friction is reduced in areas around the vertical oscillation amplitude maxima.

At 19 dBm, friction has vanished exactly at the wave field (vertical) maxima. The hysteresis gets locally more pronounced, but also narrower. On both sides of the point of

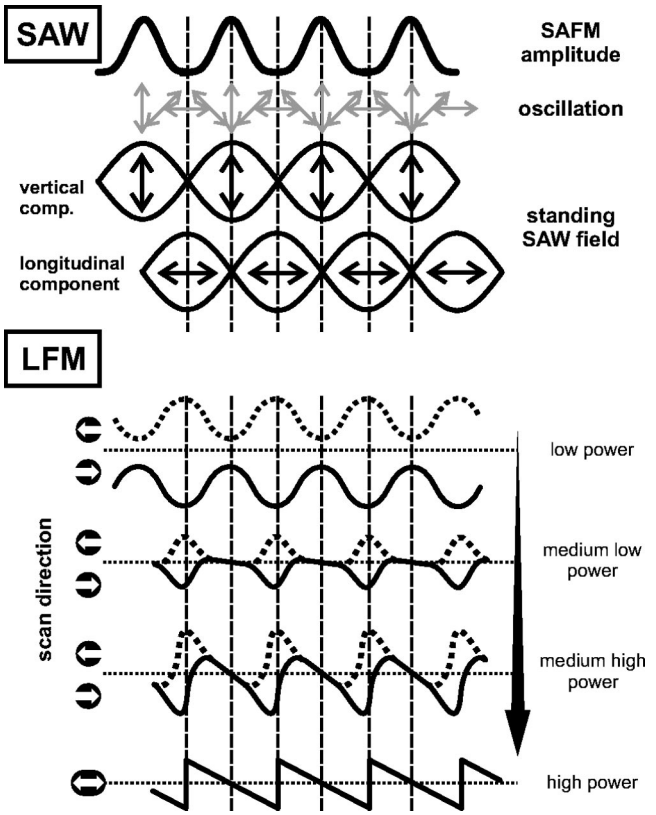

FIG. 7. Upper part: standing SAW field showing vertical and lateral oscillation components. Lower part: corresponding LFM response for increasing wave amplitude. At low power, friction is locally reduced at the points of high wave amplitude. At medium low power, friction vanishes at these points. The scan direction-independent signal shows a slight slope, which enhances significantly at medium high power. At the wave amplitude nodes, the hysteresis is still clearly visible. At high power, friction as well as the hysteresis are completely suppressed.

zero friction, additionally, a scan direction-independent slope appears. The stronger modulation of the LFM traces underlines the nonlinear character of the underlying mechanism, i.e., the mechanical diode effect.

At 22 dBm, the hysteresis is almost completely suppressed. The modulation is now smaller than at low rf power. Furthermore, the underlying scan direction-independent signal gets a maximum added to the slope close to the wave node positions.

At 24 dBm, only the scan direction-independent signature remains in both traces. The points of zero friction are still at the positions of the wave field antinodes and the peaks, that appeared clearly from about 22 dBm on, are now almost right at the positions of the wave field nodes.

B. Qualitative discussion

Figure 7 shows a sketch of the different wave amplitude-dependent regimes of the LFM signal for scanning over a standing Rayleigh wave field. In the upper half, the SAW related traces, and below, the corresponding LFM responses are shown. Assuming a standing Rayleigh wave field, the maxima of the vertical oscillation component are repeating every $\lambda/2$ and are shifted with respect to the maxima of the longitudinal component by 90°. The amplitude ratio of both oscillation components can be calculated numerically for any given material system (about 5:3 in this case). At the nodes of the wave field (i.e., the nodes of the vertical component of the standing wave field), guides to the eye are drawn throughout the sketch. When scanning along the wave field, the tip encounters a continuous transition of the surface movement from a purely vertical movement to a purely longitudinal movement and so forth. The uppermost trace shows the SAFM amplitude signal. It is obtained as the demodulation of the vertical rf surface movement via the mechanical diode effect. It exhibits, as the exploited force-distance curve is a nonlinear function, a slightly deformed sinusoidal shape.

In the lower half of the sketch, the response in the LFM signal is exemplified. From analyzing the experimental data, roughly four power regimes can be distinguished: at low power, friction is locally reduced at the points of high wave amplitude, i.e., large vertical oscillation components. The resulting LFM hysteresis is thus reduced in these areas, as described by the friction reduction effect. At medium low power, friction is then locally completely suppressed. However, the LFM signal, which is at these positions identical for both scanning directions, shows a slight slope. The point of zero friction remains right on the point of maximum vertical oscillation. At medium high power, the slope increases and, around the wave amplitude nodes, the reduced hysteresis remains clearly visible. Its position coincides with the maximum of the longitudinal wave component, i.e., the point of pure lateral oscillation.

Then at high power, the hysteresis is completely suppressed. The remaining scan direction-independent traces exhibit maxima close to the positions of the wave field nodes. The points of zero friction are now right on the wave field node and around the antinode positions. Looking at points in the vicinity of the longitudinal oscillation maxima, it is obvious that the increasing vertical oscillation components lead, via the rectifying effect of the mechanical diode, to a net force on the cantilever pointing towards the positions of the longitudinal oscillation maxima. On the other hand, in the area around the maxima of the vertical oscillation component, it is obvious that the forces point away from this area. The cantilever will thus experience effective forces that pull in the direction of the longitudinal maxima and push away from the positions of the vertical maxima (as can be seen from the SAFM amplitude trace). Thus, lateral forces with alternating sign (and a periodicity of $\lambda_{SAW}/2$) act on the cantilever, when scanning over the standing wave field. This mechanism thus appears as a *lateral rectification* of the longitudinal component of the standing wave field.

In an ideal case, i.e., 100% standing wave field modulation, friction will not vanish at the nodes of the standing wave field (vanishing vertical oscillation component), independent from the applied power. However, in our setup, the wave amplitude modulation is not perfect. Thus, the remaining propagating SAW field component is high enough (in the high power limit) to lead to a complete suppression of friction throughout the wave field. This also leads to the rounded and slightly deformed shape of the measured LFM traces where, to a first approximation, a sawtooth-like behavior is

expected at the positions of the vertical oscillation minima (compare Fig. 6, lower trace, and Fig. 7, lower trace).

VI. CONCLUSIONS

In conclusion, we demonstrated the effect of local friction reduction due to the ultrasonic surface oscillations driven by surface acoustic waves. This effect was measured on a variety of surfaces for ultrasonic frequencies ranging from 200 MHz to 3 GHz. Employing crossed standing acoustic wave fields, the amplitude dependence of the effect could be studied without varying the measurement conditions within a single scan. With increasing SAW amplitude friction is reduced, and above a certain threshold amplitude, friction vanishes completely. Taking the SAFM measurements of the position of the vertical and longitudinal wave field nodes into account, the effect could clearly be pinpointed to the vertical oscillation component. Also, measurements of purely in-plane polarized Love waves showed no friction reduction effect. This leads us to the conclusion that most probably the mechanical diode effect, i.e., the effective shift of the slowly responding cantilever off of the surface due to rf surface vibrations, is responsible for the reduced friction. This was additionally confirmed by the investigation of the amplitude-dependence of the down-converted SAW amplitudes in standard SAFM and LFM–SAFM. In a regime where friction within a standing wave field was locally completely suppressed, low frequency vertical cantilever oscillations are observed, whereas lateral or torsional oscillations are not excited. The mechanism of friction reduction gives an elegant explanation for this effect. The investigation of the large SAW amplitude response of the LFM signal lead to the finding of the lateral rectification effect. It can be stringently explained by a very simple model, also containing the lubrication effect for the lower power regime.

Future experiments in a controlled humidity environment, together with absolutely calibrated wave amplitudes, will open up a way for perfectly controlled friction variation. We hope that this method will further stimulate research on the fundamentals of friction, with implications from technologically relevant systems down to the study of atomic point contacts. In particular, we believe that ultrasound will be of great importance for solving some of the tribological obstacles of microelectromechanical systems.[18]

ACKNOWLEDGMENTS

The authors gratefully acknowledge the technical assistance of W. Seidel and K. Hauck, and R. Koch for critically reading the manuscript. G.B. would like to thank the DAAD and T.H. thanks the Deutsche Akademie der Naturforscher, Leopoldina, and the DFG for their financial support.

[1] H. D. Fridman and P. Levesque, J. Appl. Phys. **30**, 1572 (1959).
[2] R. Pohlman and E. Lehfeldt, Ultrasonics **4**, 178 (1966).
[3] D. Godfrey, ASLE Trans. **10**, 183 (1967).
[4] H.-J. Jungclaus, Ph.D. thesis, RWTH Aachen, 1973 (in German).
[5] F. Dinelli, S. K. Biswas, G. A. D. Briggs, and O. V. Kolosov, Appl. Phys. Lett. **71**, 1177 (1997).
[6] V. Scherer, W. Arnold, and B. Bhushan, Surf. Interface Anal. **27**, 578 (1999).
[7] ThermoMicroscopes, model M5.
[8] ThermoMicroscopes, ultralevers.
[9] G. Meyer and N. M. Amer, Appl. Phys. Lett. **57**, 2089 (1990).
[10] C. M. Mate, G. M. McClelland, R. Erlandsson, and S. Chiang, Phys. Rev. Lett. **59**, 1942 (1987).
[11] M. Liley *et al.*, Science **280**, 273 (1998).
[12] T. Hesjedal, E. Chilla, and H.-J. Fröhlich, Appl. Phys. A: Mater. Sci. Process. **61**, 237 (1995).
[13] W. Rohrbeck and E. Chilla, Phys. Status Solidi A **131**, 69 (1992); O. Kolosov and K. Yamanaka, Jpn. J. Appl. Phys., Part 2 **32**, L1095 (1993).
[14] T. Hesjedal, E. Chilla, and H.-J. Fröhlich, in *1996 Ultrasonics Symposium Proceedings* (IEEE, New York, 1996), p. 811; E. Chilla, T. Hesjedal, and H.-J. Fröhlich, Phys. Rev. B **55**, 15852 (1997).
[15] G. Behme, T. Hesjedal, E. Chilla, and H.-J. Fröhlich, Appl. Phys. Lett. **73**, 882 (1998).
[16] G. Behme and T. Hesjedal, Appl. Phys. A: Mater. Sci. Process. **70**, 361 (2000).
[17] (unpublished).
[18] B. Bhushan, *Tribology Issues and Opportunities in MEMS* (Kluwer, Boston, 1997).